



Materials Impact on the Performance Analysis and Optimization of RF MEMS Switch for 5G Reconfigurable Antenna

K. Srinivasa Rao¹ · P. Naveena¹ · K. Girija Sravani^{1,2}

Received: 10 January 2019 / Revised: 16 April 2019 / Accepted: 14 June 2019 / Published online: 3 July 2019
© The Korean Institute of Electrical and Electronic Material Engineers 2019

Abstract

In this paper, we have enhanced the performance of the existing switch operating at 35 GHz by using a novel optimization process and these results are compared with the existing experimental results. The same optimization process is utilized to design the switch at 5G mobile communication frequencies (38 GHz) and its performance is analyzed. The switch is designed on the coplanar waveguide having 50 Ω impedance matching and is optimized based on the wireless application system for Ka-band (27–40 GHz) at a resonance frequency of 38 GHz. The proposed switch at 38 GHz exhibits low input reflection coefficient (S_{11}) of 13.86 dB (> 10 dB), low insertion loss (S_{12}) of 0.44 dB (< 1 dB) and high isolation (S_{21}) of 33 dB at Ka-band frequencies. The proposed structure is designed to have less spring constant of 2.38 N/m and actuation voltage of 11.97 V. During UP state position switch develops an ON-state capacitance of 31 fF and OFF state capacitance of 0.152 pF during downstate with a capacitance ratio of 4.90. The switch requires low switching time of 0.19 ms and it can withstand up to the force of 12.97×10^{-4} N which is generated during actuation. Thus, the proposed switch can be effectively optimized for good performance and can be used for high-frequency 5G communication applications.

Keywords RF MEMS Switches · Pull-In Voltage · Capacitance · Switching time · Isolation · Insertion · Return Loss

1 Introduction

Radiofrequency micro electro mechanical systems (RF MEMS) Technology is a promising technology for communication system because of low loss and high performance. In present years, intense research in MEMS technology devices and its fabrication has been attracted many researchers, academicians, and industrialists towards communication field. There is a great demand for smaller and faster communication systems which need less area and low power consumption [1]. Radio frequency micro electro mechanical systems (RF MEMS) have been dominating and replaced the

existing conventional solid-state semiconductor devices such as pin diodes, field effect transistors, etc. These RF MEMS devices are innovative especially in switch design, where the design size varies from 1 to 100 μm . Katehi et al. [2] RF MEMS switches are classified as follows, based on the actuation mechanism: (1) electrostatic, (2) magneto static, (3) piezoelectric, (4) thermal. Depends on the type of contact with the signal line: resistive type or capacitive type, In-circuit configuration perspective: Series type and Shunt type, based on the mechanical movement of the beam either in vertical or lateral movement: Fixed Fixed Beam and Cantilever Beam.

These switches are mainly used in reconfigurable antennas to change its electrical length and frequency characteristics by activating and deactivating the antenna elements. MEMS switches can be used for high-frequency applications in which switch function is based on mechanical movement of the beam. The actuation of MEMS switches has investigated by many types of research since. The first MEMS device switch is fabricated in 1979 by Petersen. The eminent research work brought a rapid development in RF MEMS and it can be efficiently used for Ka-band frequency

✉ K. Srinivasa Rao
srinivasakarumuri@gmail.com

✉ P. Naveena
naveenanavee3993@gmail.com

¹ Department of Electronics and Communications Engineering, MEMS Research Centre, Koneru Lakshmaiah Education Foundation, Greenfields, Vaddeswaram, Guntur, Andhra Pradesh 522502, India

² National MEMS Design Center, National Institute of Technology, Silchar, Silchar, Assam 788010, India

of (27–40 GHz) for 5G, Satellite communications, and military aircraft applications [3].

Roh et al. reported, the development in the field of telecommunication through improvising the research, particularly in Long Term Evolution (LTE) enhancement techniques like multiple input multiple outputs (MIMO), co-ordinate multipoint (CoMP), heterogeneous networks (HetNets) has been able to manage the traffic requirement for the next few years. The telecommunication industry and the academic institutions have been delivering significant outcomes in fourth generation (4G) LTE to deliver high data rates to the consumers by increasing the number of base stations, merging of spectra, etc. But none of the processes has been able to solve the hurdle of managing the traffic urge estimated for 2020. Hence 5G technology has come into existence. For this 5G technology, wide bandwidths method is proposed. In this patch antenna is take as 3 GHz and at 30 GHz an array antenna is used at communications [4]. Keller et al. proposed a method for decreasing the weight of the total system and minimize the complexity of wafer-scale fabrication. In this, a coplanar waveguide fed with a patch antenna for satellite communication purpose. It is designed to operate at ka-band (27–40 GHz) frequency band having a return loss of 10 dB [5]. Rahim et al. proposed A new ideology for reconfigurable antennas has been implemented with two different configurations i.e. narrowband to narrowband and wideband to narrowband in microstrip antenna and slot type antenna for wireless communication mainly for millimeter wave 5G technology [6]. Hong et al. mentioned the first-time practical solution design considerations for effective results are achieved by the phased-array mesh-grid antenna with dual-polarized beam switching for human cellular handsets. This technology can lead to the experience of an mm-Wave 5G radios designed in a Smart Phone, it is designed at a frequency of 60 GHz to integrated with reconfigurable antenna [7]. Demirel et al. [9] presented the breakdown of the bridge type RF-MEMS switches occur due to the deformation caused by the thermal expansion. In this switch having an actuation voltage of 25 V and isolation less than 20 dB and can be operated at 28–40 GHz frequency band. Hence, it is minimized by the inclusion of anchors to the device design. Korany et al. presented in detail about the dual-band circularly polarized phase antenna was designed for mobile communication which can be operated at 28–38 GHz having a reflection coefficient of -15 dB and gain greater than 7 dB and an axial ratio less than 3 dB. This can deliver radiation performance such that it does not affect the head-hand proximity of the user. The designed antenna structure can be able to fit in the sleek mobile device and it may be able to use the design in millimeter wave 5G applications [8].

To overcome the drawbacks and to improve the functionality we have proposed an optimization process for the switch structure based on the frequency of application which

improves the performance of the switch, in terms of high isolation and low insertion loss and less pull in voltage. The proposed process is step by step from down to top approach. For the proposed method firstly, we extract the dimensions of the switch and done some electromechanical analysis and RF performance of the switch and compared our results with the existing fabricated measured results. During the comparison we have observed that our extracted optimized switch performance is approximately same and it requires less pull in voltage. Thus, if anyone want to go for fabrication directly can through optimization process and extract the required dimensions, then these dimensions can be used for fabrication which indirectly helps in cost effectiveness. The impedance matching depends on the substrate height and material for the substrate and coplanar waveguide. The coplanar waveguide dimensions are fixed based on the impedance matching of 50Ω . The signal line should possess less transmission loss to transmit the RF input signal, so that isolation will be increased and loss of signal transmitting also decreased (return and insertion loss). The pull-in voltage depends on the actuation area and spring constant. The spring constant is directly related to the dimensions of the beam which are length, width, and thickness of the beam. The overlapping area also depends on the dimensions of the beam. By increasing the overlapping area pull in voltage will be reduced. To extract the dimensions of the beam and dielectric an optimization step by step process is followed to get well suitable dimensions. By this, the proposed switch can be operated at high frequencies applications and it can be integrated with an antenna for wireless communications in 5G technology.

The rest of the Paper organized in different sections. In Sect. 2 optimization applied for an existing switch, the proposed switch complete design, optimization process, device working, and dimensions are presented. In Sect. 3 the electromechanical analysis in that capacitance and pull in voltage and spring constant, stress analysis and C–V characteristics, Eigen frequency, RF performance of the switch are discussed. In Sect. 4 the comparison of the performance of new switch with the base paper.

2 Device Optimization and Its Specifications

2.1 Optimization Process

The proposed RF MEMS capacitive shunt switch is designed for 5G wireless applications. The device dimensions are fixed based on the parameters Such as impedance matching, Up capacitance and resonant frequency. The switch is designed using FEM tools and performance is enhanced to work at ka-band frequency range. The RF MEMS capacitive shunt switch mainly contains substrate, coplanar waveguide,

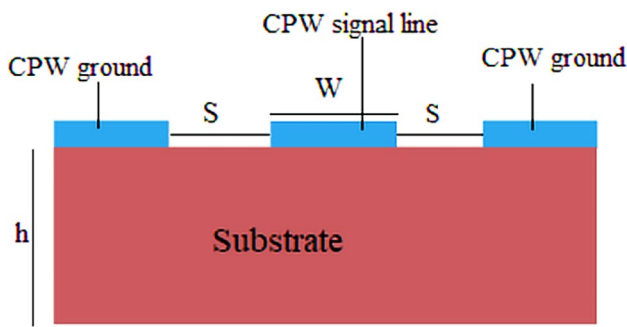


Fig. 1 A schematic view of substrate and CPW

the dielectric layer, actuation electrodes, and bridge membrane. Initially, to design a switch at frequency there should be an impedance matching of 50Ω to allow the RF input signal through the coplanar waveguide. The impedance matching Z_0 depends on the spacing between the ground plane and width of the signal line, height of the substrate and dielectric constant of the substrate material (Fig. 1).

The height of the substrate can be estimated condition is

$$\frac{h}{\lambda} > 0.33 \tag{1}$$

where h represents the height of the substrate, λ is wavelength. The wavelength of the radiating signal line is obtained by

$$\lambda = \frac{C}{F_C} \tag{2}$$

C is the velocity of light in vacuum $C = 3 \times 10^8$ m/s and F_C is the cut off frequency.

The maximum height of the substrate can be calculated from Eq. 1. The cutoff frequency of the waves given by the formula below

$$F_C \leq \frac{nC}{4h\sqrt{\epsilon_r - 1}} \tag{3}$$

where n is the order of transmission mode and C is the velocity of light in a vacuum ϵ_r is the relative dielectric constant of the substrate material and H is the height of the substrate and f_c is the cut off frequency.

The height of the substrate is taken from the above calculation and CPW contains a signal line and ground planes on either side of the signal line. The spacing (S) between the ground and signal line and the width of the signal line is evaluated for impedance matching [17]. The pull-in voltage depends on the actuation area of the bridge. The actuation or overlapping area of the bridge can be calculated as $A = W \times w$, such that W and w is the width of the signal line and bridge respectively. The width of the bridge is

determined from the upstate capacitance and the resonant frequency of the switch [16]

$$F_r = \frac{1}{2\pi\sqrt{LC_U}} \tag{4}$$

where F_r is the resonant frequency which is 38 GHz and $L = 0.4$ nH developed by the CPW transmission line and C_U is the upstate capacitance.

The up capacitance of the switch is, [19]

$$C_U = \frac{\epsilon_o A}{g + \frac{t_d}{\epsilon_r}} \tag{5}$$

where $\epsilon_o = 8.825 \times 10^{-12}$ F/m, $A = W \times w$, g is a gap between the beam and dielectric at actuation area and t_s is the thickness of the dielectric and ϵ_r is a relative dielectric constant of beam material. By solving the above equation w is the width of the beam is obtained and the length of the beam is four times of its width i.e. $L = 3$ or $4 \times w$.

The buckling effect depends on the thickness of the bridge and can be estimated through the formula

$$g > \frac{4\sqrt{2}}{3} t \tag{6}$$

Here g is the gap between the bridge and CPW, based on the gap there will be a high capacitance ratio and better displacement of the beam. The beam displacement highly depends on its thickness (Fig. 2).

2.2 Optimization for 35 GHz

The optimization process is applied to the existing switch proposed by Chu et al. and the enhancement in its performance by optimization process is analyzed for validation. Chu et al. proposed a fixed–fixed switch at the 35 GHz

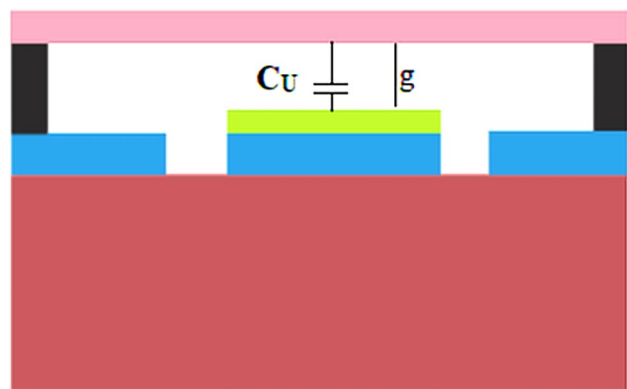
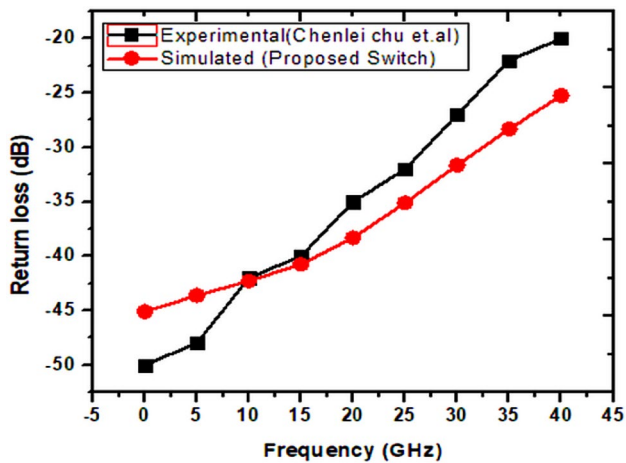


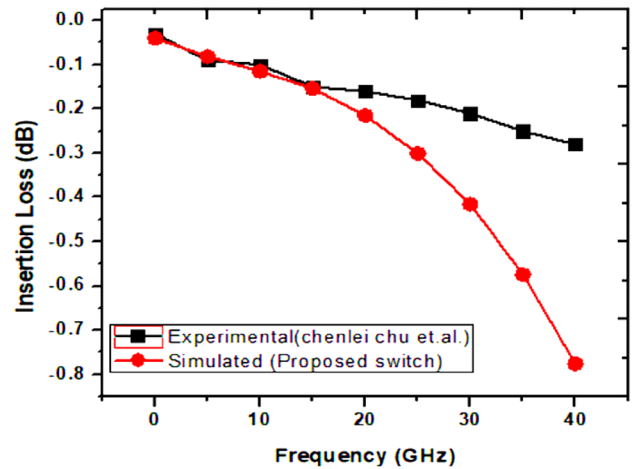
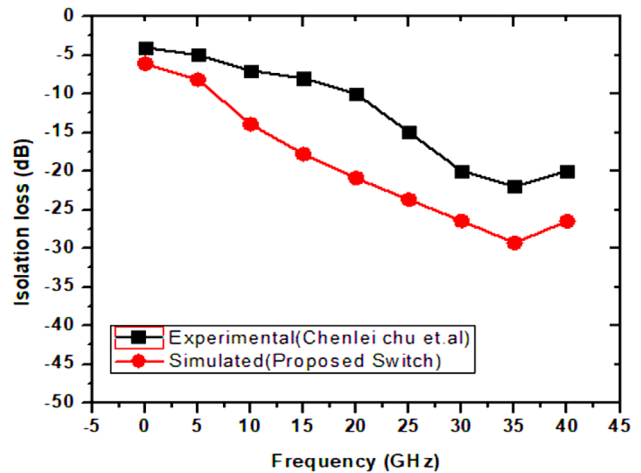
Fig. 2 Capacitance in Upstate position of the proposed switch

Table 1 Specific dimensions of MEMS capacitive switch

Indicator	Elements	Dimensions
G/S/G	Coplanar waveguide	56 μm /95 μm /56 μm
H	Substrate height	400 μm
W	The width of membrane bridge beam	186 μm
L	Length of a membrane bridge beam	745 μm
g_0	Air gap	3 μm
t_d	Dielectric thickness	0.2 μm
As	Square holes	6 μm \times 6 μm
A	Actuation area	186 μm \times 745 μm

**Fig. 3** Return loss comparison of the proposed switch with an existing switch

frequency by T matching techniques for impedance matching of 50ohms and the switch dimensions, performance electromechanical analysis and fabricated switch measured values. Here we applied our optimization process to the same fixed-fixed switch and enhanced performance characteristics are compared with the Chu et al. switch. By using this optimization process follows the design of RF MEMS switch on CPW with impedance matching of 50 Ω . The dimensions of the switch are changed with respective of length, width, thickness, and gap. The pull-in voltage is reduced through this optimization and performance of the switch is also approximately increased. The pull voltage is reduced to 9.67 V from 36 V and the isolation is increased to -29 dB from -20 dB at 35 GHz. The optimized dimensions for 35 GHz are shown in Table 1 and its performance analysis graphs are presented from Figs. 3, 4 and 5. The same optimization process is applied for 38 GHz operation frequency such that electromechanical analysis and S-parameter analysis are carried out for understanding switch performance.

**Fig. 4** Insertion loss comparison of the proposed switch with an existing switch**Fig. 5** Isolation loss comparison of the proposed switch with an existing switch

Return loss is nothing but reflection loss of the RF input signal at the input terminal, it should be less. In Fig. 3, we compared our simulation results with the existing experimental results to show the performance of our proposed optimization process. We have observed at 10 GHz it is having an approximately equal return loss of -42.2883 dB. At the operating frequency 35 GHz our simulated result shows -28 dB whereas experimental is having -20.4 dB.

Insertion loss is nothing but the loss of RF input signal at the input terminal while the signal is inserting into the signal line, it should be in between 0 and -1 dB. From Fig. 4, we can observe our optimized design model simulation exhibiting better results when compared with the existing experimental results. At operating frequency 35 GHz it is having > 1 dB, in some cases, both are having the same

insertion loss. So we can suggest our proposed process is exhibiting better results.

Isolation loss is nothing but blocking of RF input signal between the input and output ports, it should be high. We compared our simulation results with the existing experimental results which are graphitized in Fig. 5 it shows the performance of our proposed optimization process. For simulation result, it is having isolation of -29 dB at 35 GHz when compared with experimental results it exhibits -25 dB at 35 GHz (Table 2).

2.3 Optimization for 38 GHz

The proposed RF MEMS switch is fixed fixed type switch such that both ends of the beam are fixed and the electrostatic actuation is applied at the center of the beam. The capacitance is developed between the beam and a signal line. SiO_2 layer is deposited over the substrate. The coplanar waveguide is constructed having two ground planes and a signal line. The dielectric layer is taken over the signal line to develop capacitance between the signal line and Beam Bridge of $0.2 \mu\text{m}$ thick dielectric is deposited over the signal line. The perforations are created inside the beam to reduce stiction problem, easy movement of the bridge and to reduce the pull-in voltage. Two actuation electrodes are constructed under the beam, over the SiO_2 layer provides an electrostatic force to deflect the beam downwards.

Initially, the switch is in ON state which transmits the signal without any deflection in the beam. When a potential difference is applied to the beam, it gets deflected toward down so that it breaks down on dielectric layer enabling OFF condition. The voltage at which the beam breaks down when it undergoes $2/3$ rd displacement is called pull-in voltage. The switch is modeled by using electro-mechanics physics in COMSOL Multiphysics tool such that the behavior of the switch to the applied voltage and capacitance is generated between the electrodes

is studied by observing the displacement of the bridge in the vertical z-direction; it shows the switch is in ON state. The main motto of RF MEMS switches is required less pull in voltage and better performance. Solid mechanics physics is applied to simulate the switch and understand the buckling effect. The robustness of the switch and the tensile strength of the material used for the beam can be analyzed. The performance of the switch is verified by using HFSS tool (Fig. 6; Table 3).

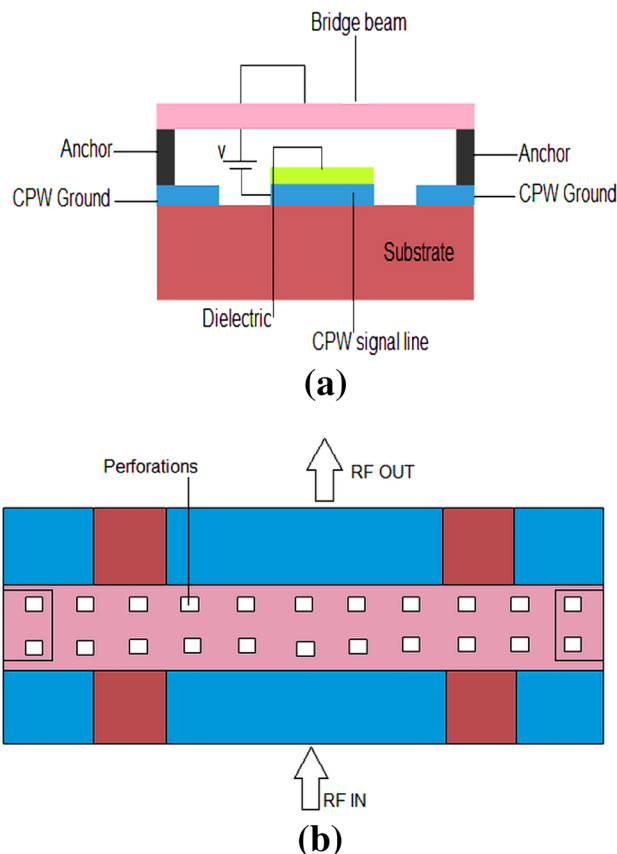


Fig. 6 Schematic view of the proposed switch. **a** Side view, **b** top view

Table 2 Comparison of the proposed switch with Existing switch

Parameters	Chu et al. [2] 2017 at 35 GHz	Optimization 35 GHz
Spring constant	–	1.717 N/m
Pull in voltage	36 V	9.36 V
ON capacitance	–	423 fF
OFF capacitance	–	0.0368 pF
Capacitance ratio	–	1.508
Substrate material	Gallium Arsenide (GaAs)	Silicon(Si)
Beam material	Gold(Au)	Aluminum(Al)
Return loss	-20.4 dB	-28 dB
Insertion loss	<1 dB	<1 dB
Isolation loss	25 dB	29 dB

Table 3 Specific dimensions of MEMS Capacitive switch

Indicator	Elements	Dimensions
G/S/G	Coplanar waveguide	$56 \mu\text{m}/95 \mu\text{m}/56 \mu\text{m}$
H	Substrate height	$400 \mu\text{m}$
W	Width of membrane bridge beam	$186 \mu\text{m}$
L	Length of membrane bridge beam	$745 \mu\text{m}$
g_0	Air gap	$3 \mu\text{m}$
t_d	Dielectric thickness	$0.2 \mu\text{m}$
As	Square holes	$6 \mu\text{m} \times 6 \mu\text{m}$
A	Actuation area	$186 \mu\text{m} \times 745 \mu\text{m}$

2.4 Material Selection

In designing a device, material selection plays a key role in the functioning and performance of the device and the cost for fabrication of the device. RF MEMS switch performance turned depends on the material selection. From the past decades, different strategies have proposed based on their properties. Rao proposed a selection methodology for materials in graph and matrix form, but it is more complex in computational. R. Roth suggested a multi-attribute utility analysis (MAUA) which is more time-consuming. Ashby's furnished less computational material selection strategy. For RF MEMS switch Ashby approach is extensively in practice for material selection of beam, dielectric, and substrate [10]. Noted the all possible materials which are suitable for the component. Extract all properties limits and material indices and then screened the materials based on its ranking. Plot the graph based on material indices between the properties unbiased graph is developed, from that graph the left most material is suitable for the switch compared to other considered materials.

Here we considered all possible materials suitable for substrate and scattered the graph against Poisson's ratio versus young's modulus. From Fig. 7, the left and topmost material Si (Silicon) shows high Young's modulus and low Poisson's ratio is taken as the substrate material. Material with high Young's modulus possess high stiffness layer and lightly placed. Impedance matching depends on the dielectric constant of the material of substrate which improves the performance of the switch. Silicon is chosen as the material for the substrate because of its high resistivity, less cost and having phase velocity of silicon is 3.44. The transmitting of signal loss is low due to its high dielectric constant $\epsilon_r = 11.9$. Secondly, the most important is co-planar

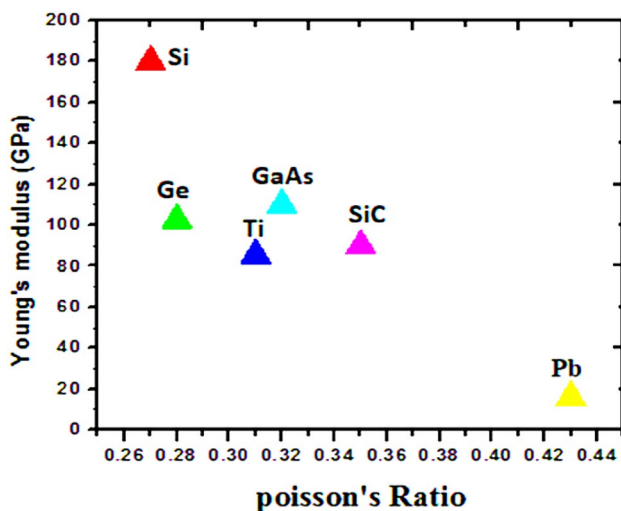


Fig. 7 Material selection for the substrate of switch

waveguide dimensions which plays a prominent role in RF signal transmission.

All possible materials which are suitable for the dielectric layer are taken and plotted the graph over variation between the dielectric constant and electrical resistivity. The material with a high dielectric constant with moderate resistivity is taken as a dielectric layer. From Fig. 8 HfO_2 (Hafnium oxide) is chosen as the dielectric layer, due to high dielectric constant. The pull-down capacitance will be increased with a dielectric constant of the material which directly depends on the capacitance ratio of the switch, with increasing the capacitance ratio and pull-down capacitance and the charging and stability of the switch will be maintained.

All possible materials suitable for beam material are considered and plot the graph with their indices variation between Young's modulus and Poisson's ratio. The material with low Poisson's ratio and moderate young's modulus is taken as beam material. From Fig. 9 among the materials plotted above Al is having Young's modulus not too high but not too low, so that the stiffness in the beam is flexible but not too hard. Then in the movement or bending of the beam is flexible. So, it is considered as best beam material. The Al (Aluminum) is less costly compared to Au (Gold).so here we took Al as the beam material (Table 4).

3 Results and Analysis for 38 GHz

3.1 Electromechanical Analysis

3.1.1 Pull in Voltage

The pull-in voltage or actuation voltage is defined as the voltage required by the beam to pull down towards the electrode and shows minimum 2/3rd displacement in the gap

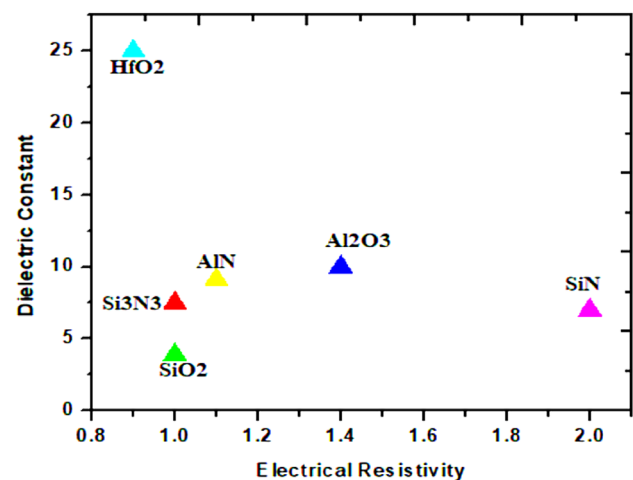


Fig. 8 Material selection for the dielectric of switch

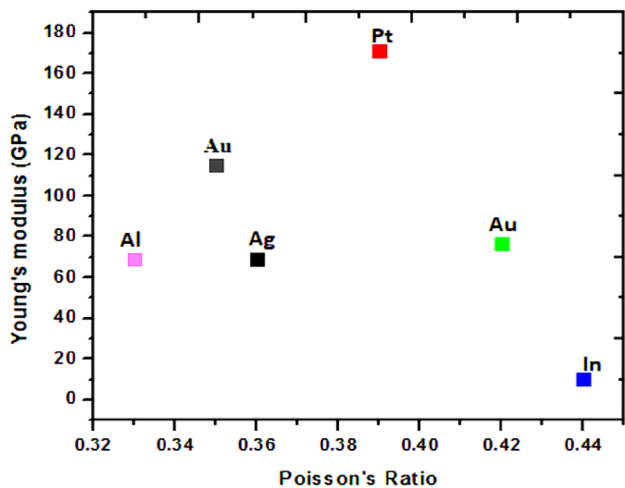


Fig. 9 Material selection for a beam of switch

Table 4 Material selection for proposed RF MEMS switch

Selection	Material
Substrate	Silicon (Si)
Coplanar wave guide	Aluminum (Al)
Dielectric layer	Hafnium oxide (HfO ₂)
Anchors	Aluminum (Al)
Fixed fixed beam	Aluminum (Al)

between the beam and down electrode. The pull-in voltage of the beam can be calculated by using [11]

$$V_p = \sqrt{\frac{8Kg^3}{27\epsilon_0 A}} \text{ Volts} \tag{7}$$

Here k is the spring constant [20]

$$K = \frac{32Ewt^3}{L^3} \tag{8}$$

where g is a gap between the electrode and beam, ϵ_0 permittivity in free space; an actuation area i.e. is the width of the signal line and w is the width of the beam. $A = W \times w$. The pull-in voltage is measured as 11.97 V and the spring constant is 2.406 N/m (Fig. 10).

From Fig. 11 we can observe that there is a constant displacement of the beam after the pull in voltage of 11.97 V through Comsol simulations. Here in this, all simulation data which is performed through the finite element method is plotted the graph over voltage versus displacement. From Fig. 12 the maximum displacement is occurred at the center of the beam. The pull voltage is directly proportional to power consumption, with less pull in voltage there will be less power consumption and fast switching time.

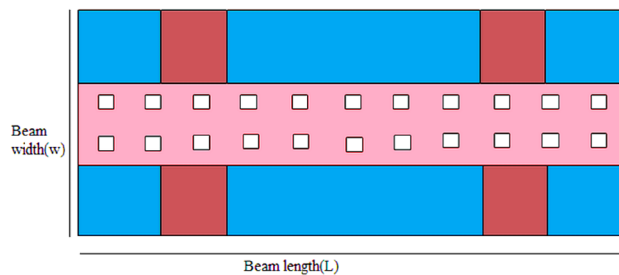


Fig. 10 Proposed beam structure

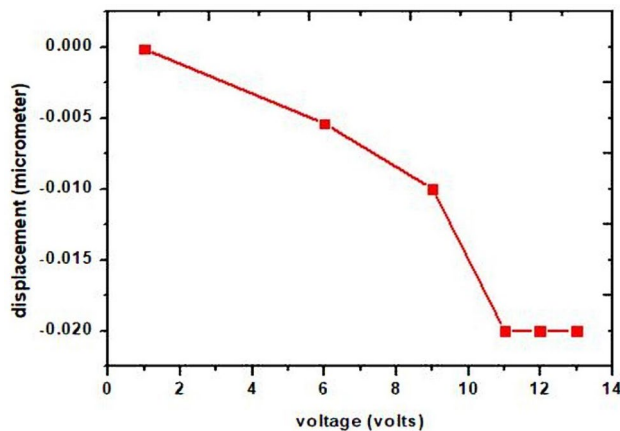


Fig. 11 Voltage versus displacement

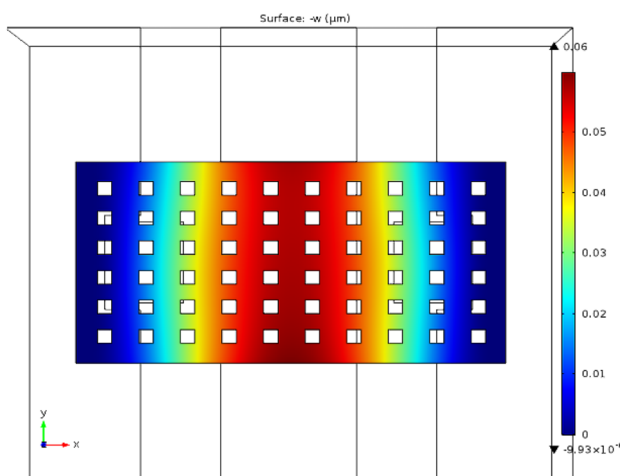


Fig. 12 Displacement of a beam for voltage

3.1.2 Switching Time Analysis

The switching time is defined as the time taken to change its position from one state to another state, that time taken by the device is called switching time or switching speed. The switching speed of the switch would be low then it can be

work fast. The switching time of the RF MEMS shunt switch can be given as [12]

$$T_s = \frac{3.67V_p}{V_s\omega_0} \text{ Seconds} \tag{9}$$

where V_p —pull-in voltage, V_s —supply voltage, $V_s = 1.4V_p$. ω_0 represent resonant frequency. Then switching time required by the switch is $t_s = 0.19$ ms.

The resonant frequency can be calculated from the effective mass and spring constant

$$\omega_0 = \frac{1}{2\pi} \sqrt{\frac{K}{m}} \text{ Hertz} \tag{10}$$

$$\omega_0 = 13.70 \text{ kHz.}$$

From Fig. 13 it illustrates the speed of switch, how the beam is actuating for applied source voltage and the graph plotted against the switching time and source voltage. For pull in voltage 11.97 V it is having switching time of 0.19 ms.

3.1.3 ON or UP State Capacitance (C_{ON})

In capacitive shunt switch, it is initially in ON state when the voltage is applied to the beam the membrane gets displaced downwards and capacitance is developed between the electrode and beam. It is ON capacitance or Upstate capacitance. The Upstate Capacitance C_{ON} is calculated as [13]

$$C_{ON} = \frac{\epsilon_o\epsilon_rxy}{g + \frac{t_d}{\epsilon_r}} \text{ F} \tag{11}$$

$$C_{ON} = 31 \text{ fF}$$

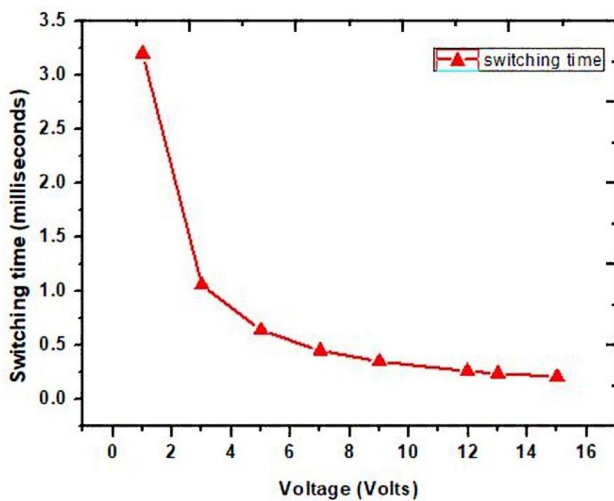


Fig. 13 Source voltage versus switching time

x —width of the beam, y —length of the beam, g —gap between dielectric and beam, t_d —the thickness of the dielectric, ϵ_r —relative permittivity of beam material (Table 5).

Here graph is plotted between the simulated and theoretical upstate capacitance of the switch. The upstate capacitance mainly depends on the gap between the electrodes where as gap is inversely proportional to the upstate capacitance, with increase in gap the capacitance will be decreased. The upstate capacitance is also depends on the dielectric thickness. Here we observed from the Fig. 14 that for various gaps its is having different capacitances in On condition. We considered 3 μ m gap because in point of fabrication and also to reduce the stiction problem so the upstate capacitance obtained is 31 fF through finite element method. We observed approximately same for theoretical and simulated values in COMSOL tool.

3.1.4 Down or OFF State Capacitance (C_{OFF})

The capacitance developed by the switch when the gap vanishes due to a displacement of the beam during actuation is called down state capacitance. The obtained capacitance is termed as downstate or off state capacitance which offers a high impedance to transmit the signal to the output terminal.

C_{off} is the downstate capacitance it can be calculated as

$$C_{OFF} = \frac{\epsilon_o\epsilon_rxy}{t_d} \text{ Farad} \tag{12}$$

Table 5 ON State Capacitance

Gap (g)	ON capacitance (C_{ON})	
	Simulated (fF)	Calculated (fF)
1 μ m	762	775
2 μ m	399	412
3 μ m	31	44

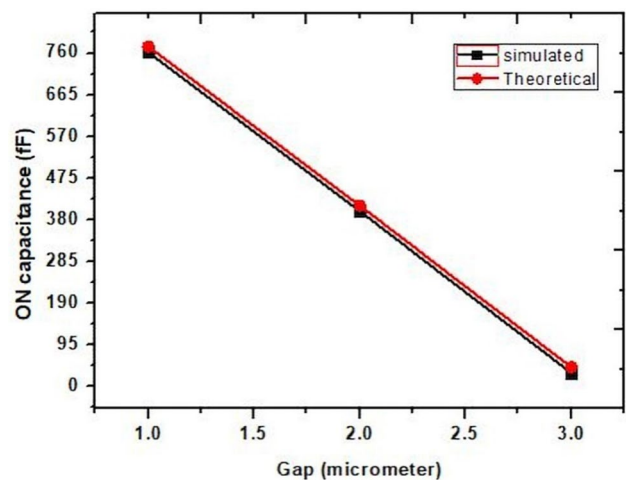


Fig. 14 Simulated and theoretical at UP state

$$C_{OFF} = 0.152 \text{ pF.}$$

In this, from Fig. 15 there is little deviation between the simulated and theoretical. The down state capacitance mainly depends on the dielectric thickness of the switch, which is inversely proportional to the downstate capacitance. Here graph is plotted between the simulated and theoretical downstate capacitance of the switch. Here we considered 0.2 μm as the dielectric thickness and downstate capacitance obtained is 0.152 pF through finite element method (Table 6).

By observing the above graph Fig. 16, if the voltage increases the capacitance developed between the bottom electrode and beam membrane also increases gradually, there is a uniform increase in capacitance up to some supply voltage but when it reaches the pull-in voltage, the beam gets 2/3rd deflection over the gap between them. Then capacitance developed is known as upstate capacitance.

3.1.5 Capacitance Ratio (C_{ratio})

It is defined as the ratio of the Downstate capacitance (OFF state) and Upstate capacitance (ON state) of the proposed switch.

$$C_{ratio} = \frac{C_{OFF}}{C_{ON}} = 104.09 \tag{13}$$

3.1.6 Stress Analysis

Finite element modeling tools are used to observe and analyze the performance of the switch in respective aspects. In COM-SOL Multiphysics, solid mechanics is used to observing the stress distribution over the beam membrane of the switch for an applied force. Here aluminum is taken as the beam material.

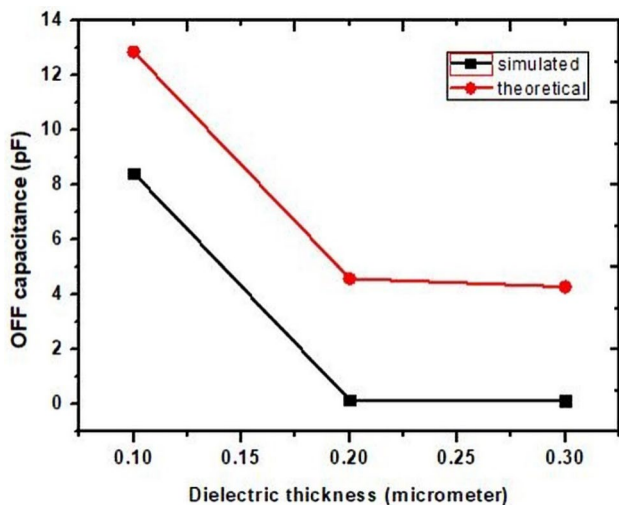


Fig. 15 Simulated and theoretical at DOWN state

Table 6 OFF state capacitance

Dielectric thickness (t_d)	OFF capacitance (C_{OFF})	
	Simulated (pF)	Calculated (pF)
0.1 μm	8.438	12.86
0.2 μm	0.152	4.58
0.3 μm	0.134	4.28

The aluminum can exhibit 70 MPa of stress, for maximum force $12.97E^{-4}$ N. The switched beam can be affording maximum force based on its tensile strength of a material. The electrostatic force is induced on the beam when the voltage is applied. The electrostatic force is given by [21]

$$F = \frac{QE}{2} \tag{14}$$

Hence charge $Q = CV$

$$F = \frac{CVE}{2} \tag{15}$$

An electric field $E = \frac{V}{g}$, g is the gap between the beam bridge and down electrode (Fig. 17).

$$F = \frac{CV^2}{2g} \tag{16}$$

Considering the Parallel plate capacitance (Fig. 18), the capacitance is

$$C = \frac{\epsilon_0 \epsilon_r A}{g} = \frac{\epsilon_0 \epsilon_r Wl}{g} \tag{17}$$

$$F = \frac{\epsilon_0 \epsilon_r V^2 A}{2g^2} \text{ Newton} \tag{18}$$

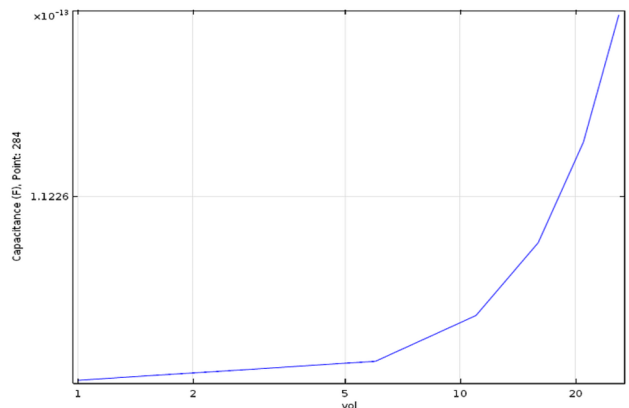
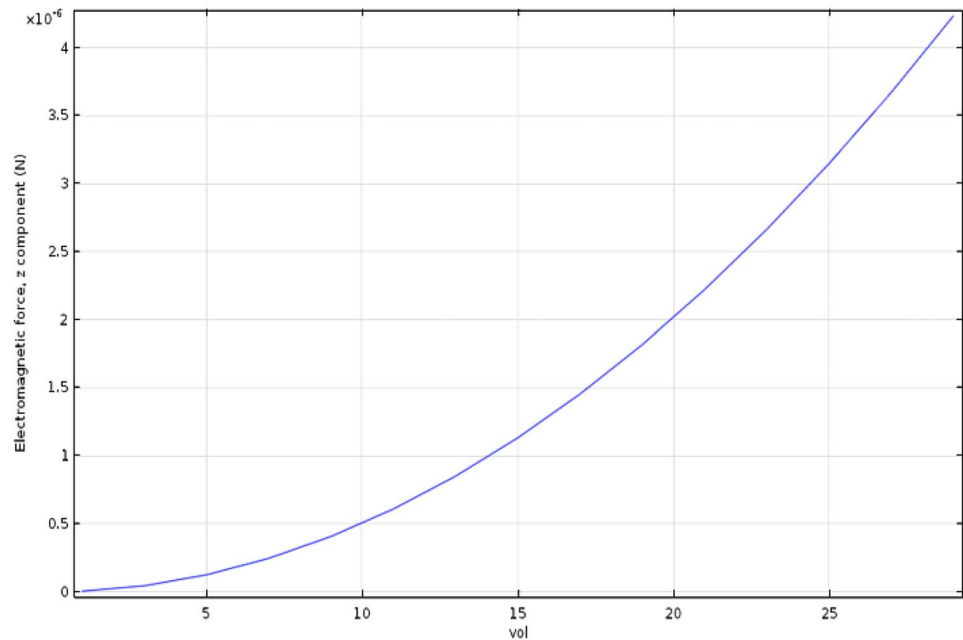


Fig. 16 Capacitance versus voltage

Fig. 17 Voltage versus magnetic force



3.1.7 Eigen Frequency Analysis

Eigen frequency analysis is observed by using FEM tools. In this analysis, the vibration of the membrane in a particular frequency and motion of the membrane is in a vertical direction (Fig. 19) [18].

3.1.8 Power Handling

Power handling is an important factor in MEMS technology, the MEMS devices consume less power compared to pin diodes and semi conductor's switches. The RF MEMS shunt

switch required very less power to work; mainly it depends on actuation voltage of the switch. The power consumption of shunt switch can be given by [15].

$$P = \frac{V_P^2}{Z_o} = 2.38 \mu\text{w} \quad (19)$$

3.2 RF Performance Analysis of Shunt Switch

RF performance of the switch can be analyzed by using HFSS tool and operating frequency can be analyzed [14]. Return loss is the loss of RF signal during transmission reflected back at the input terminal due to impedance mismatching of the switch. The reflected back signal is called a reflection coefficient. The return loss or reflection coefficient can be observed when the switch is in ON state. The reflection coefficient should be < -10 dB. It can be denoted as S_{11} . The return loss at 38 GHz frequency ka band is -13.086 dB (Fig. 20).

$$S_{11} = -20 \log \left[\frac{VSWR - 1}{VSWR + 1} \right]$$

$$VSWR = \frac{1 + \gamma}{1 - \gamma} \quad (20)$$

$$\gamma = \frac{Z_o - Z_L}{Z_o + Z_L}$$

Insertion loss has occurred during RF signal is transmitting. It is due to resistive loss in switch or contact of a beam with metal. Insertion loss either the switch is in ON state or OFF state (Fig. 21).

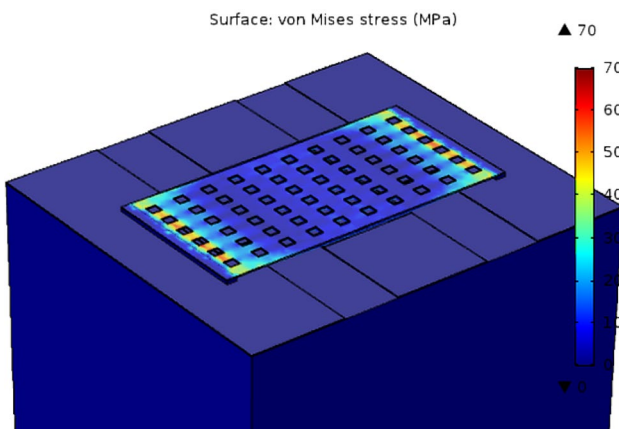


Fig. 18 Stress distribution

Fig. 19 Vertical vibration for Eigen frequency

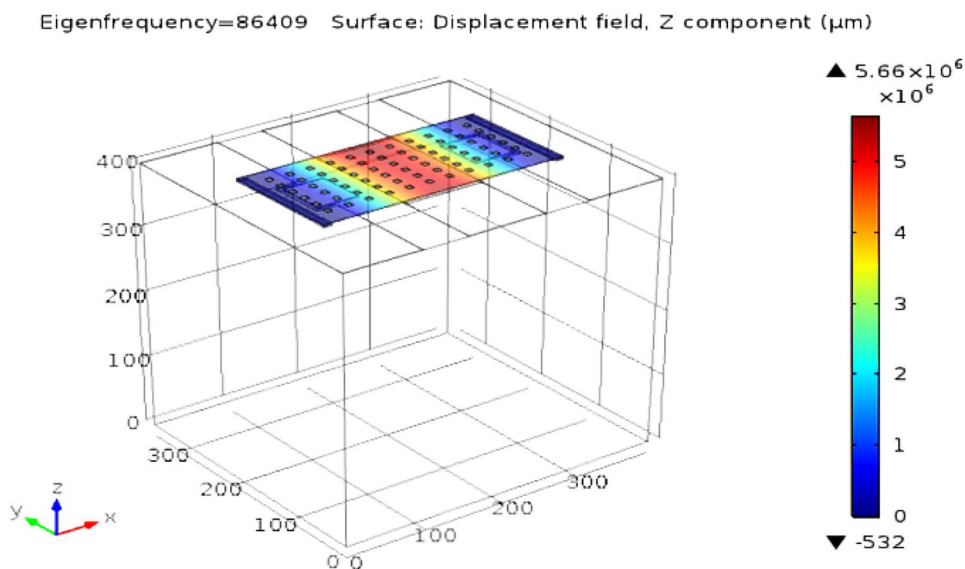
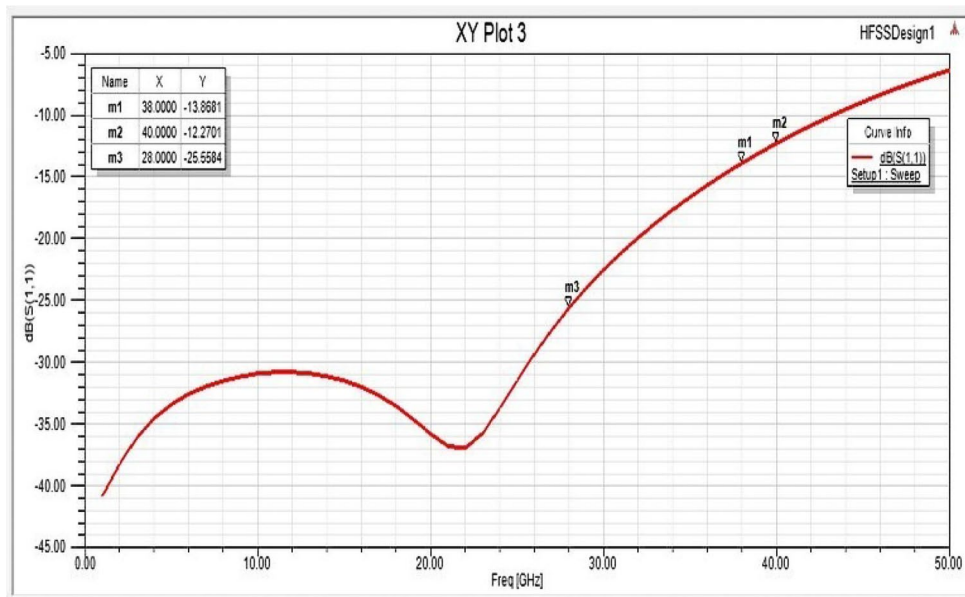


Fig. 20 Return loss of proposed switch in HFSS



$$S_{12} = 20 \log \left[\frac{Z_A + Z_B + Z_C}{Z_A + Z_B} \right] \tag{21}$$

Isolation should be high for the high-frequency application it is nothing but blocking of the signal between the input and output signal terminals of the switch. It can occur when capacitive coupling happens between the beam and electrode. It should be less than $|-10 \text{ dB}|$. It can be denoted as S_{21} . The isolation of proposed at 38 GHz is 31 dB (Fig. 22; Table 7).

$$S_{21} = 20 \log \left| \frac{2R_b}{2R_b + Z_0} \right| \tag{22}$$

4 Conclusion

In this paper, A novel optimization model is proposed and is applied to the switch at 35 GHz which is fabricated by Chu et al. The dimensions of the fabricated switch are altered using the optimization process and performance results are compared with the existing results. The optimized is exhibits high-performance characteristics such as low pull in voltage 9.36 V and isolation -29 dB then the fabricated switch. Hence the optimization process is performed to design a fixed-fixed type switch at operating

Fig. 21 The insertion loss of proposed switch in HFSS

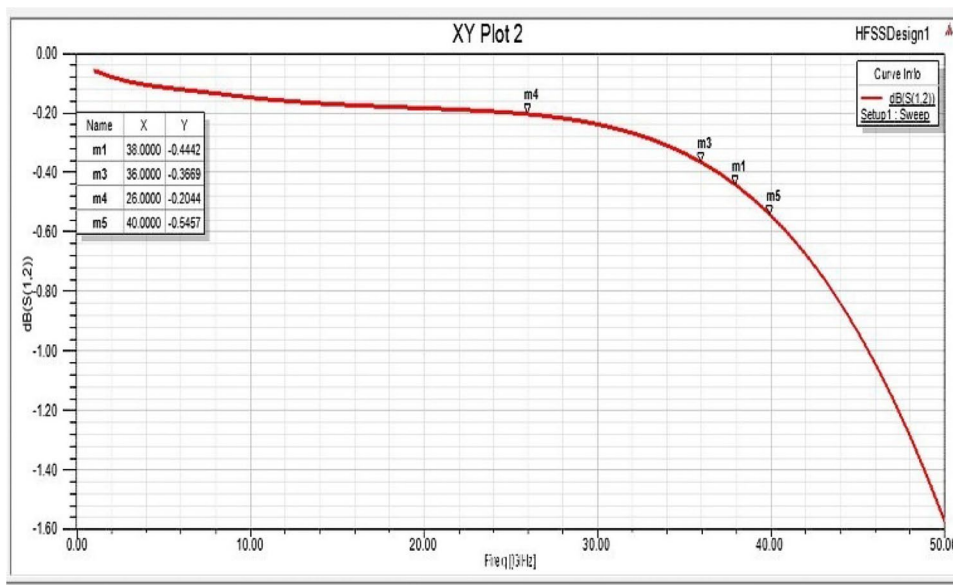


Fig. 22 Isolation of proposed switch in HFSS

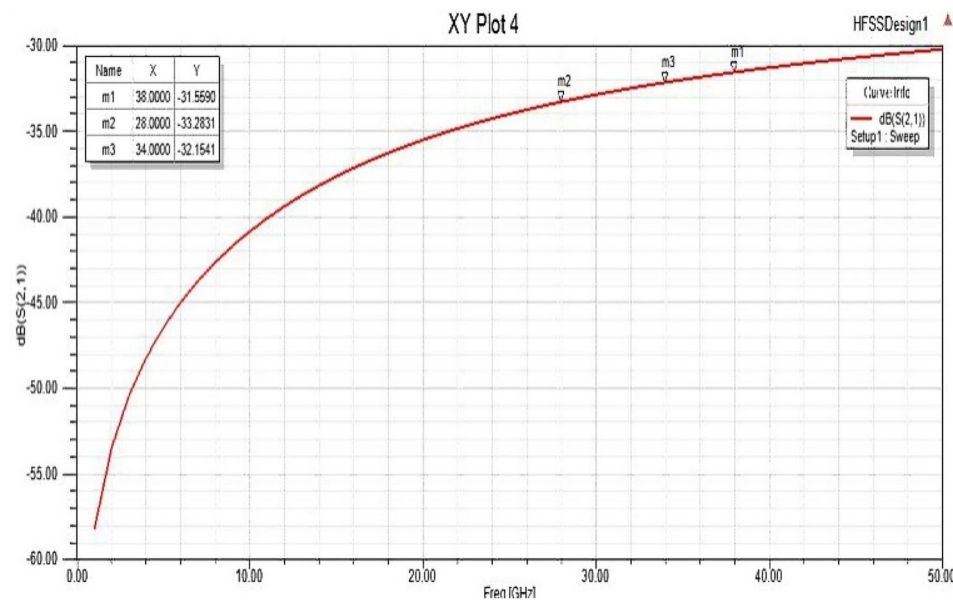


Table 7 Proposed RF MEMS Switch Optimization Analysis

Parameter	Optimized switch 38 GHz	Muldavin [22] 22–38 GHz	Demirel et al. [9] 28–40 GHz
Spring constant	2.38 N/m	–	–
Pull in voltage	11.97 V	15–25 V	22 V
ON capacitance	31 fF	–	–
OFF capacitance	0.152 pF	1.5 pF	–
Switching time	0.19 ms	–	–
Power consumption	2.8 μw	–	–
Insertion loss	< 1 dB	< 0.3–0.6 dB	< 0.35 dB
Return loss	– 13 dB	< – 20 dB	< – 15 dB
Isolation loss	– 31 dB	45–50 dB	37 dB

frequency of 38 GHz. The switch produces high isolation of -31 dB actuating at the pull-in voltage of 11.97 V with a spring constant of 2.38 N/m which is obtained by the optimization process. The electromechanical analysis such as Upstate, Downstate capacitances, C–V characteristics and stress analysis have been carried out. The performance of the switch is analyzed by taking appropriate materials selected by Ashby's approach. These optimized dimensions are feasible to fabricate. These types of switches can be efficiently used as the switch element between the patches of the antenna for reconfigurability at high frequencies and can be utilized in future 5G communication applications.

Acknowledgements The authors would like to thank NMDC, supported by Government of India, for providing necessary design facilities through NPMAS.

References

1. T.S. Rappaport, Y. Xing, G.R. MacCartney, A.F. Molisch, E. Melios, J. Zhang, Overview of millimeter wave communications for fifth-generation (5G) wireless networks—with a focus on propagation models. *IEEE Trans. Antennas Propag.* **65**(12), 6213–6230 (2017)
2. C. Chu, X. Liao, H. Yan, Ka-band RF MEMS capacitive switch with low loss, high isolation, long-term reliability and high power handling based on GaAs MMIC. *IET Microw. Antennas Propag.* **11**(6), 942–948 (2017)
3. L.P.B. Katehi, J.F. Harvey, E. Brown, MEMS and Si micromachined circuits for high-frequency applications. *IEEE Trans. Microw. Theory Tech.* **50**(3), 858–866 (2002)
4. W. Roh, J.-Y. Seol, J. Park, B. Lee et al., Millimeter-wave beam forming as an enabling technology for 5G cellular communications: theoretical feasibility and prototype results. *IEEE Commun. Mag.* **52**(2), 106–113 (2014)
5. S.D. Keller, Coplanar waveguide slot-coupled Ka-band patch antenna for integration with wafer-scale beam-steering MEMS control board. *ACES J.* **23**(2), 1054–4887 (2008)
6. M.K.A. Rahim, M.R. Hamid, N.A. Samsuri, et al., Frequency reconfigurable antenna for a future wireless communication system, in *46th European Microwave Conference (EuMC), London, UK, 4–6 Oct 2016*
7. W. Hong, K.-H. Baek, S. Ko, Millimeter-wave 5G antennas for smartphones: overview and experimental demonstration. *IEEE Trans. Antennas Propag.* **65**(12), 6250–6261 (2017)
8. K.R. Mahmoud, A.M. Montaser, Design of dual-band circularly polarized array antenna package for 5G mobile terminals with beam-steering capabilities. *IET Microw. Antennas Propag.* **12**(1), 29–39 (2017)
9. K. Demirel, E. Yazgan, S. Demir, T. Akin, A new temperature-tolerant RF MEMS switch structure design and fabrication for Ka-band applications. *J. Microelectromech. Syst.* **25**(1), 60–68 (2016)
10. A.K. Sharma, *Design, Simulation, and Analysis of RF-MEMS Switches for Reconfigurable Antennas* (Birla Institute of Technology and Science, Pilani, 2014)
11. K.S. Rao, P. Ashok Kumar, K. Guha, K.L. Baishnab, K.G. Sravani, Design and simulation of fixed-fixed flexure type RF MEMS switch for the reconfigurable antenna. *Microsyst. Technol.* (2018). <https://doi.org/10.1007/s00542-018-3983-2>
12. K.S. Rao, P. Naveena, T.V. Aravind Swamy, Design and performance analysis of self-similar reconfigurable antenna by cantilever type RF MEMS switch. *Microsyst. Technol.* (2019). <https://doi.org/10.1007/s00542-019-04370-x>
13. T. Lakshmi Narayana, K.G. Sravani, K.S. Rao, Design and analysis of CPW based shunt capacitive RF MEMS switch. *Cogent Eng.* **4**(1), 1–9 (2017)
14. J.B. Muldavin, G.M. Rebeiz, High-isolation CPW MEMS switches, part 2: design. *IEEE Trans. Microw. Tech.* **48**(6), 1053–1056 (2000)
15. G.M. Rebeiz, *RF MEMS: Theory, Design, and Technology*, 1st edn. (Wiley, New York, 2003)
16. S. Molaei, B.A. Ganji, Design and simulation of a novel RF MEMS shunt capacitive switch with low actuation voltage and high isolation. *Microsyst. Technol.* **23**(6), 1907–1912 (2016)
17. R. Simons, *Coplanar waveguide circuits, components, and systems*. (Wiley, 2001), pp. 15–21. <https://www.microwaves101.com/calculators/864-coplanar-waveguide-calculator>.
18. K. Srinivasa Rao, P.A. Ashok Kumar, K.G. Sravani, Performance analysis of series: shunt configuration based RF MEMS switch for satellite communication applications. *Microsyst. Technol.* (2018). <https://doi.org/10.1007/s00542-018-3907-1>
19. S. Molaei, B.A. Ganji, Design and simulation of a novel RF MEMS shunt capacitive switch with low actuation voltage and high isolation. *Microsyst. Technol.* **23**(6), 1907–1912 (2013)
20. T. Sharma, A. Tyagi, Review of mechanical modeling of fixed-fixed beams in RF MEMS switches, in *Third International Conference on Advanced Computing and Communication Technologies (ACCT) (2013)*
21. O. Pertin, Pull-in-voltage and RF analysis of MEMS-based high-performance capacitive shunt switch. *Microelectron. J.* **77**, 5–15 (2018)
22. J.B. Muldavin, G.M. Rebeiz, High-isolation CPW MEMS shunt switches—Part 2: design. *IEEE Trans. Microw. Theory Tech.* **48**(6), 1053–1056 (2000)

Publisher's Note Springer Nature remains neutral with regard to jurisdictional claims in published maps and institutional affiliations.